Payri, R.; Salvador Rubio, FJ.; Gimeno, J.; Peraza, JE. (2016). Experimental study of the injection conditions influence over n-dodecane and diesel sprays with two ECN single-hole nozzles. Part II: Reactive atmosphere. Energy Conversion and Management. 126:1157-1167. doi:10.1016/j.enconman.2016.07.079.

Experimental study of the injection conditions influence over n-dodecane and diesel sprays with two ECN single-hole nozzles Part II: Reactive atmosphere

Raul Payri[a], F. J. Salvador[a], Jaime Gimeno[a,*], Jesús E. Peraza[a]

[a] *CMT - Motores Térmicos, Camino de Vera (s/n), Universitat Politècnica de València, Edificio 6D, 46022, Valencia, Spain.*

Abstract

The second part of this experimental analysis, presented in this paper, seeks to go deep on the characterization of the Spray C and Spray D nozzles from the Engine Combustion Network, investigating the penetration of fuel spray at reacting conditions alongside characteristic parameters of combustion such as ignition delay and lift-off length. Both ECN mono-orifice injectors have similar nozzle flow capacity but different conicity degrees and corner sharpness, being Spray C more susceptible to cavitate. Schlieren imaging technique was employed to quantitatively measure reactive penetration and ignition delay, while lift-off length was identified through OH* chemiluminescence. As in the inert part of this research, n-dodecane and commercial diesel were selected for the tests, thereby the effect of the fuel properties in the measured parameters was analyzed. Also, once again the concept of *R-parameter*, defined as the penetration derivative respect to the square root of time was calculated to delve into the penetration behavior. The experiments were performed in a constant pressure-flow facility able to reproduce engine-like thermodynamic conditions. Results revealed that *R-parameter* evolution can be divided in four stages: an inert zone, a 'bump', a 'valley' part and a quasi-steady one that overlaps the previous inert part. Those stages are highly governed by ambient temperature and oxygen concentration. Nozzle geometry and fuel properties demonstrated to have a noteworthy influence on all measured parameters.

Keywords: Fuels, ECN Nozzles, Schlieren, Chemiluminescence, Tip penetration, Lift-off length, Ignition delay

1. Introduction

Enhancement of the exhaust pollutant emissions control in diesel engines is a global and ever growing concern, which has concentrated efforts worldwide of researchers and engine designers [1–3]. A matter of special interest within this field is the injection system due to the fundamental role played by the fuel spray atomization and mixture preparation until ignition delay in the combustion efficiency and emissions formation. These processes are largely linked to key parameters that can be related with the environment where fuel is injected or with the injection system technology and performance [4].

To study the spray evolution and combustion phenomenon experimentally, facilities capable of recreating the in-cylinder conditions of a thermal engine and allowing optically visualize the internal processes, are necessary. Many research centers have acquired facilities of this kind and have carried out several experiments which has greatly increased the amount of data in this area, but that does not necessarily make it easily comparable between institutions that have worked with different laboratory frameworks [5–7].

In this context, Engine Combustion Network (ECN) [8] is an international open forum which promotes the collaboration among experimental and computational scientists in engine combustion field, in order to provide them a coherent database of experimental and numerical results with high reliability and accuracy. With this

* Corresponding author. E-mail address: jaigigar@mot.upv.es.

Cite as:

Payri, R., Salvador, F.J. Gimeno, J. and Peraza, J.E., "Experimental study of the injection conditions influence over n-dodecane and diesel sprays with two {ECN} single-hole nozzles. Part II: Reactive atmosphere", *Energy Conversion and Management*, (2016), Vol. 126, pp. 1157–1167. doi:10.1016/j.enconman.2016.07.079

Nomenclature

Acronyms

ASOE	After start of energizing
ASOI	After start of injection
CMOS	Complementary metal-oxide-semiconductor
CPF	Constant-pressure flow (facility)
CWL	Central wave length
ECN	Engine Combustion Network
ICCD	Intensified charge-coupled device
nDod	n-Dodecane (abbr. used in plot legends)
PID	Proportional–integral–derivative controller
SoCF	Start of cool flames
SSI	Second stage of the ignition
TTL	Transistor-transistor logic
U.V.	Ultraviolet

Variables

D	Diameter
ID	Ignition delay
$k\text{-}factor$	Conicity factor used in industry
LOL	Lift-off length
$\dot{M}$	Spray momentum
p	Pressure
R	*R-parameter*
Re	Reynolds number
S	Penetration
T	Temperature
t	Time
u	Velocity
y	Total intensity of spray pixels
Z	Mixture fraction

Greek Symbols

Δp	$p_{rail} - p_{amb}$
Δy	Increment of spray intensity
ρ	Density
θ	Spreading spray angle

Subscripts

$_{100}$	Total distillation (temperature)
$_{amb}$	Ambient condition
$_{inj}$	Injection property at nozzle exit
$_{o}$	Of the nozzle outlet
$_{rail}$	In rail - of injection (pressure)
$_{sto}$	Stoichiometric
$_{v}$	Vapor phase

objective, Robert Bosch GmbH and Delphi Automotive Systems have donated to ECN injectors with identical nominal characteristics [9] which are used by experimentalists to characterize the spray and combustion behavior employing their different facilities [6, 7] and standardized measure methods at reference tightly-controlled tests conditions.

In the literature, macroscopic visualization of diesel sprays has been widely employed to perform spray penetration measurements. Similar trends of reactive penetration with operation conditions have been observed in Refs. [10, 11]. Schlieren imaging has proved itself to be a valuable technique to investigate both reactive and inert sprays penetrations [12, 13], determining generally the faster spray expansion in presence of combustion. This technique has been also employed for ignition delay measurements under the knowledge of the light intensity characteristics of each combustion phase [14, 15]. Furthermore, several authors have underlined the effect of air–fuel mixture on soot formation, which can be associated with lift-off length [16–19]. It has been determined that ambient oxygen concentration rises products effective temperature, which continues increasing reactant temperatures and consequently reducing the ignition delay time [20]. On the other hand, Pickett et al. concluded in [21] that high temperature combustion products created during the premixed burn, keep having influence on lift-off length. Both last two conclusions suggest a relationship between ignition delay and lift-off length, although a correlation between them is not entirely clear [20].

This document covers the second part of an investigation about the behavior of "Spray C" and "Spray D" nozzles from ECN performed in a constant-pressure flow facility (CPF) in a considerable range of operating conditions. In contrast to the first part of this research [22], the experiments shown in this manuscript were carried out in a reactive ambient ($O_2\% > 0\%$) and parameters related to combustion process as ignition delay and lift-off length were measured and analyzed besides reactive tip spray penetration. In order to investigate the influence of fuel properties, diesel and n-dodecane were used in this study.

2. Materials and proceedings

2.1. Test rig and injection system

To carry out the experiments, a constant-pressure flow test chamber capable of reproducing the diesel engines in-cylinder pressure and temperature conditions was employed. According to the convention presented by Baert et al. [5], this test rig can be classified as a constant-pressure flow (CPF) installation, due to diesel-like conditions are reached by means of a continuous gas flow at high temperature and pressure through the facility. This test

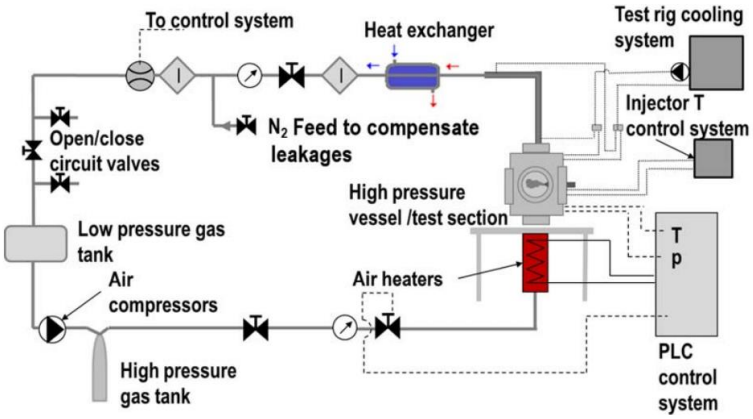

Fig. 1: Sketch of the CPF test rig employed to perform the experiments.

rig has the unique capability compared to another facilities [5, 14, 23] of obtaining nearly quiescent and steady thermodynamic conditions within the chamber, with an important reduction in the time required to perform experiments with multiple repetitions at wide ranges of conditions. In order to measure properly the temperature at the tested conditions, radiation heat transfer should be taken into account. This facility can reach operation conditions of temperature and back-pressure of 1000 K and 150 bar respectively. Fig. 1 illustrates a scheme of the test rig, which has been deeply described in [24, 25], and also in the Part I of the present research [22].

Two single-hole Bosch 3-22 injectors of the Engine Combustion Network dataset were employed to perform these experiments as in [22]. The #210003 and the #209103 nozzles were used for Spray C and Spray D respectively, according with the ECN coding reference, whose geometrical and hydraulic properties have been previously characterized and may be found in [8, 26]. The Spray C nozzle has a k-*factor* = 0 and nominal orifice diameter of 212 µm, besides a nozzle entrance with sharp corner; features that make it prone to cavitate due to the local pressure drop produced by the fillet. On the other hand, the Spray D has a k-*factor* = 1.5, a nominal diameter of 192 µm and a rounded corner entrance design to avoid cavitation.

The injection system setup consisted in connecting the injector to a common rail with a high pressure line, and fitting it in the chamber with a special injector holder that has a continous ethylene glycol flow running in a parallel circuit, so the injector nozzle tip temperature could be kept constant setting the fluid temperature [24]. The fuel was provided to the injector by a high pressure volumetric Bosch CP3 pump driven by an electric motor, and the injection pressure was set by a PID system which controls a pressure regulator in the common rail. The experiments were performed in accordance with the conditions summarized in the test matrix showed in Table 1. As in the inert part of this study [22], n-dodecane and diesel were the fuels used in the tests, whose properties are referred to in Table 2.

Table 1: Test conditions summary.

Parameter	Values	Units
Fuel[a]	n-Dodecane - Diesel	-
ECN injector label - code	C-210003 - D-209103	-
Energizing time	2.5	ms
Tip temperature	363	K
Oxygen perc. (O_2%)[a]	15 - 20.9	%(vol.)
Gas temperature (T_{amb})[a]	800 - 900	K
Gas density (ρ_{amb})[a]	22.8 - 28.8 - 35	kg/m^3
Injection pressure (p_{rail})	500 - 1000 - 1500 - 2000[b]	bar

[a] Not all Fuel - O_2% - T_{amb} - ρ_{amb} possible combinations were performed.
[b] Only for diesel tests.

Table 2: Fuel properties for n-dodecane and #2 diesel [8].

Fuel Property	n-Dodecane	Diesel	Units
T_{100}	489	623	K
Cetane number	87	46	-
Lower heat value	44.17	42.975	MJ/kg
Fuel density[a]	752.1	843	kg/m^3
Aromatics concent.	0	27	%(vol.)
Kin. viscosity[b]	1.5	2.35	mm^2/s
Flash point	356	346	K
Plot legend reference[c]	nDod	Diesel	-

[a] Value at 15 °C
[b] Value at 40 °C
[c] Name employed in plot legends due to spacing reasons

2.2. Optical techniques and setups

Table 3: Details of the optical setup for the employed techniques.

	Schlieren visualization	**OH* chemiluminescence**
Camera	Photron SA-X2	Andor-iStar
Sensor type	CMOS	ICCD
Lens diameter	100 mm	100 mm - U.V.
Diaphragm gap	4 mm	-
Filter range	$\leq$600 nm	305-315 nm CWL
Frame rate	60 kfps	1 frame per injection
Resolution	256 x 584	1024 x 1024
Shutter time	1.25 µs	-
TTL-Width	-	1.5-3 ms*
Pixel-mm	5.88	8.82
Repetitions	8	8

*Depending on the event duration.

2.2.1. Schlieren visualization

Schlieren imaging technique was employed to measure reactive vapor penetration (S_v) and ignition delay (*ID*). The schlieren single-pass setup shown in Fig. 2 was used in the same way that in [22]; the configuration is widely described by Pastor et al. [12]. A white-light 150 W halogen lamp with an incorporated diaphragm is placed at the focal length of a collimating mirror so that the rays leave the mirror being mutually parallel. The incident angle between the source and the mirror was minimized in order to reduce beam straightening. Then, the light beams are directed across the testing region. The idea of the schlieren imaging technique is that the parallel rays traveling through the spray are deviated or deflected as a consequence of the density gradients (i.e. refractive index inhomogeneities) between the spray and the hot atmosphere inside the chamber, allowing to detect the spray contour and its evolution, besides the intensity levels in the spray with time. These deviated rays are collected by a 150 mm lens with a 450 mm focal distance, where a diaphragm was located with a cut-off diameter of 4 mm. Then, the beam through a $\leq$600 µm band-pass filter just before the high-speed camera in order to reduce the combustion luminosity. Details of the optical setup can be found in Table 3.

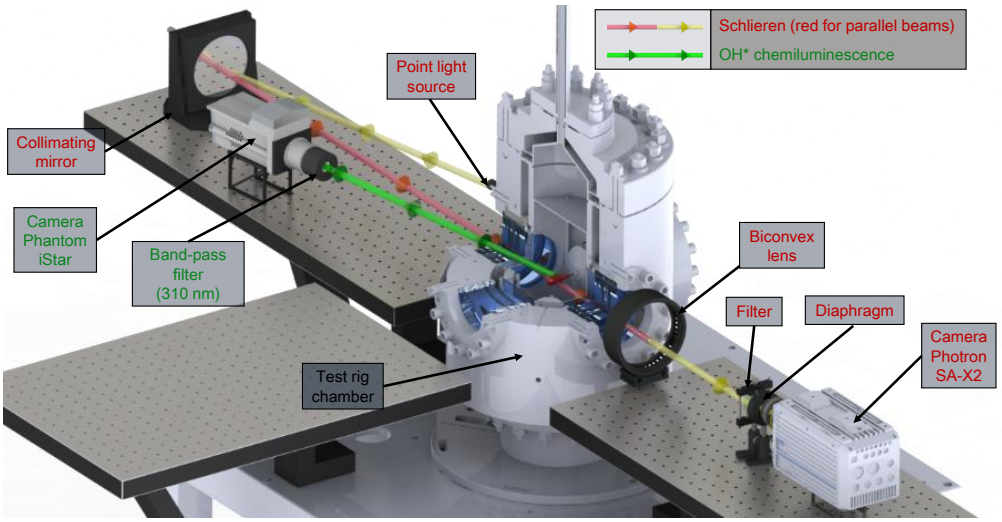

Fig. 2: Optical setup used. The main path of the light from its source to its respective camera along with the legend letters of the elements required for each technique are represented with colors.

2.2.2. OH chemiluminescence*

Chemiluminescence is defined as a light emission phenomenon resulted from a chemical reaction, commonly associated with a release of heat. Specifically, the chemiluminescence of OH* is a technique widely used in combustion investigation [14, 16, 15], in which OH* radicals are emitted when they decay at their ground state and the generated luminescence can be captured to several diagnostics as the detection of high-temperature regions or estimations of the equivalence ratio [19]. In this connection, before going further in the technique explanation, it is pertinent to define the ignition parameter that was characterized in this work using OH* chemiluminescence method: the lift-off length.

Flame lift-off is known as the distance between the tip of the injector and the zone where the combustion reaction stabilizes. According to Pickett et al. [17], this lift-off length (*LOL*) can be considered as an indicator of the time that air and fuel mixing takes before ignite, which is significantly involved in the combustion and formation of pollutants processes. Peters [27] defined lift-off length (*LOL*) as the zone where jet velocity and flame front speed stabilize at determined conditions.

OH* chemiluminescence is a valuable technique to measure the lift-off length [28, 29] due to the relationship between the heat release of a high-temperature combustion and the OH* radicals and light naturally emitted because of this chemical reaction. During the last years, several studies have used intensified cameras with interferometric filters to isolate that chemiluminescence emission to determine *LOL*. At this time, adopting the ECN standard method [16, 8], an ICCD Andor iStar camera, fitted with a 100mm f/2.8 UV lens and a 310±5 nm CWL filter was used, capturing an average image of the steady part of the combustion event and reducing the shot-to-shot deviation. The camera has a constant intensifier gating time between 2.0 and 3.2 ms after the start of the injections (ASOI) and a Transistor-Transistor Logic (TTL) signal width between 1.5 and 3 ms according to the event duration, as it has been reflected in Table 3.

2.3. Image processing

The image processing is one of the most important parts of any visualization data study [23, 30]. Images were processed using home-built software developed with the purpose of calculating the parameters following the method explained below:

2.3.1. Reactive penetration

To obtain the spray reactive penetration from schlieren images, the steps described in the first part of this investigation [22] were followed, which are also illustrated in [25]. The temporal gap between schlieren images was of $16\,\mu s$, allowing the detection of penetrations around $0.2\,\mathrm{mm}$.

2.3.2. R-parameter

Assuming a conical shaped spray at non-reacting conditions, there are some models that predict spray penetration in steady-developed regime with the form of Equation (1), considering t as time lapsed from the SOI. From this equation, it can be considered that $S_v(t) \propto \sqrt{t}$ and assuming the spray angle and the momentum flux as constants from this stabilization point [31] it is derived that the derivative of the spray penetration respect to the square root of time must be also constant. This derivative, expressed in Equation 2, has been employed in Part I of this work [22] to characterize the external flow in inert conditions and named as *R-parameter*. In that referenced study, *R-parameter* (R) showed the following advantages to analyze the spray evolution:

- *R-parameter* is independent of the spray tip position, in other words, of the past development of the spray.
- *R-parameter* is independent of time for a fully developed spray.
- Being theoretically constant, *R-parameter* allows parameterization in one only value per test $\overline{R}$.
- *R-parameter* can be correlated to other parameters, such as gas density, temperature or injection pressure.

$$S_v(t) \propto \dot{M}^{0.25} \cdot \rho_{amb}^{-0.25} \cdot \tan^{-0.5}\left(\frac{\theta_v}{2}\right) \cdot t^{0.5} \tag{1}$$

$$R = \frac{\partial S_v(t)}{\partial \sqrt{t}} \propto \dot{M}^{0.25} \cdot \rho_{amb}^{-0.25} \cdot \tan^{-0.5}\left(\frac{\theta_v}{2}\right) \tag{2}$$

Fig. 3 shows a testing sample extracted from the first part of this research [22], where the relationship between the behavior of the vapor penetration (left), and its *R-parameter* (right) and how density influences these variables are shown. There can be seen how the R exhibits a constant trend with time in its steady phase, with little experimental variability.

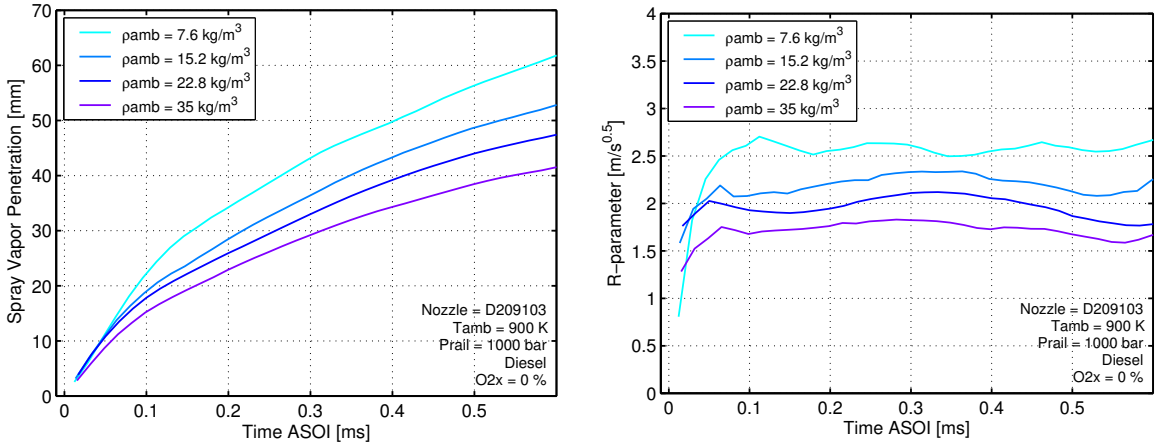

Fig. 3: Experimental example of an R-parameter calculation at inert condition [22]. Left: Vapor penetration comparison by densities of inert tests. Right: R-parameter measurements for same conditions. (Nozzle = Spray D, Fuel = Diesel, T_{amb} = 900 K, p_{rail} = 1000 bar, $O_2\%$ = 0%).

2.3.3. Ignition delay

Before giving a brief explanation of this processing method, it is appropriate to define the two main phases of diesel ignition that are characterized using this technique to study the ignition delay (*ID*).

- *Start of cool flames (SoCF)*: time interval between the start of injection and the first indication of occurrence of chemical reactions.
- *Second stage of the ignition (SSI)*: time referred to the start of injection when the high-temperature reactions start.

From schlieren imaging, the ignition delay was estimated following the methodology described by Benajes et al. in [14]. The first two steps of the procedure of image processing are the same explained before for the penetration and spreading angle (background correction and spray boundaries detection). Then, there are two parameters that are calculated:

- *Total intensity (y)*: represents the sum of each pixel that belongs to the spray.
- *Total intensity increment (Δy)*: is defined as the increment of y between two consecutive images.

With Δy computed, it is possible to observe the SoCF as a valley because of the disappearance effect, followed right after by a peak that represents the SSI due to the quick expansion and darkening of the spray as can be appreciated in Fig. 4, which compares y and Δy for two different oxygen percentages. It can be noted that image intensity increment is a suitable and robust parameter to follow the development of the ignition process. The time ASOI when the local maximum of the peak is reached is considered as the ignition delay.

2.3.4. Lift-off length

The processing of the *LOL* has been done employing the Siebers and Higgins approach [16]. Once the combustion event image is obtained and filtered with a 3x3 pixel mean filter, the flame is divided through its axis into two bottom and top profiles (Fig.5-left). The lift-off length is estimated by finding, below and above the centerline of the spray, the distances between the nozzle tip and the first axial locations which exhibit an intensity higher than a pre-selected percentage of the local peak shown in Fig.5-right, and then averaging the results of both profiles. To obtain the digital level profile, a single-average image from each repetition image was used. In Fig.5-left an example of a test sample and the *LOL* obtained employing differents percentages of the peak can

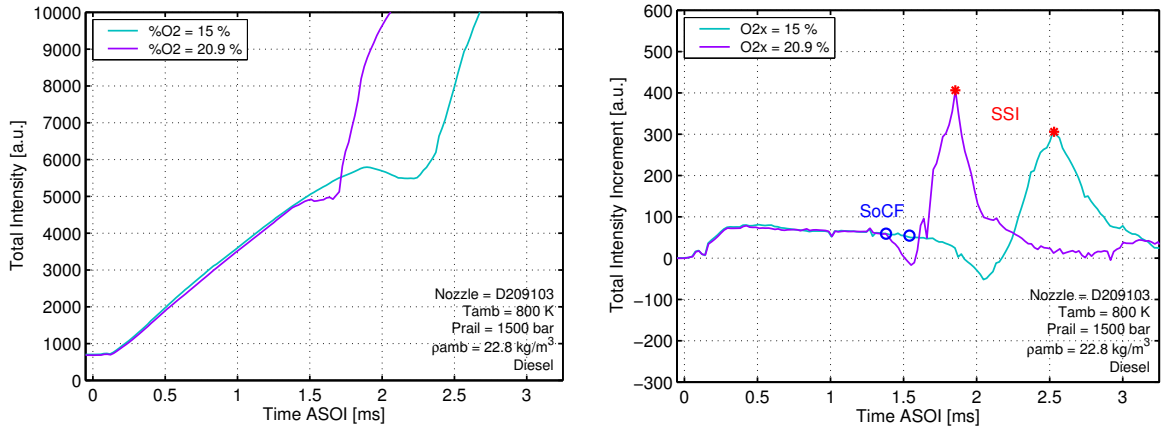

Fig. 4: Total image intensity (left) and total image intensity increment (right) for different O_2 percentages. (Nozzle = Spray D, Fuel = Diesel, T_{amb} = 800 K, ρ_{amb} = 22.8 kg/m^3, p_{rail} = 1500 bar).

be appreciated. The values reported in this work have been calculated with a 50% intensity peak percentage, following the same criteria of Benajes et al. in [14].

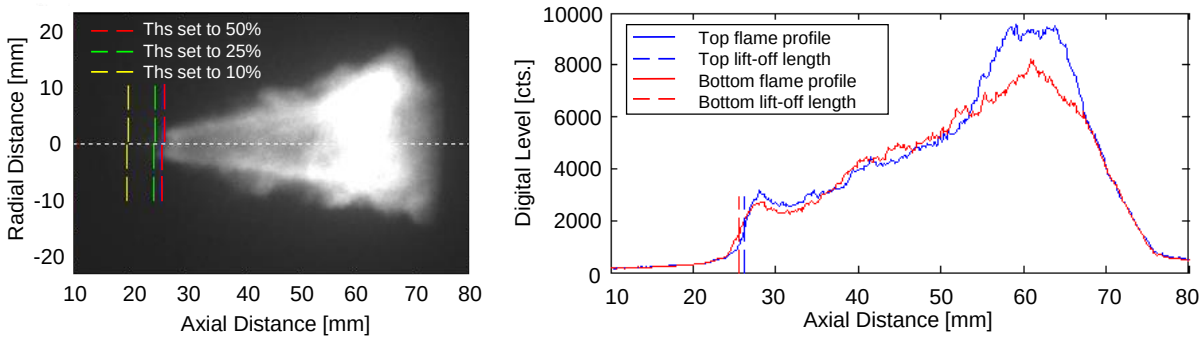

Fig. 5: Lift-off length obtained by OH* chemiluminescence. Left: raw image of one sample from the Andor iStar camera. Dashed lines represent the LOL with a 10%, 25% and 50% threshold respectively. Right: intensity profiles for bottom (continuous red) and top (continuous blue) flame sections, dashed lines of same colors represent LOL estimated with a 50% of the intensity peak. (Nozzle = Spray C, Fuel = n-Dodecane, T_{amb} = 800 K, ρ_{amb} = 22.8 kg/m^3, p_{rail} = 500 bar, O_2% = 20.9%).

3. Results and discussion

3.1. Tip penetration and R-parameter

With the aim of a better comprehension of the operating conditions effect on reactive penetration, Fig. 6 represents the penetration against the time ASOI curves varying the atmosphere density and temperature (right); and the injection pressure and oxygen concentration (left). The right plot shows the clear effect of density reducing penetration, as a result of the enlarging of the spray angle produced by the higher air entrance into the spray. This effect becomes more noticeable as the spray progresses into the chamber volume, but it is present from just after the start of the injection, to the point where ignition takes place. It is well known that temperature does not have an important influence on vapor penetration for inert sprays, as it was observed in the first part of this research [22]. However, in the reactive case illustred in Fig. 6-left, from certain moment gas temperature starts affecting greatly the reactive penetration, getting higher for tests at high temperature, due to the expansion of the spray produced by the combustion. Something similar can be appreciated in Fig. 6-right. Spray momentum increases when injection pressure is increased and consequently the penetration, which is known that occurs regardless of whether there is combustion or not. Nevertheless, it can be seen how reactive penetration is also

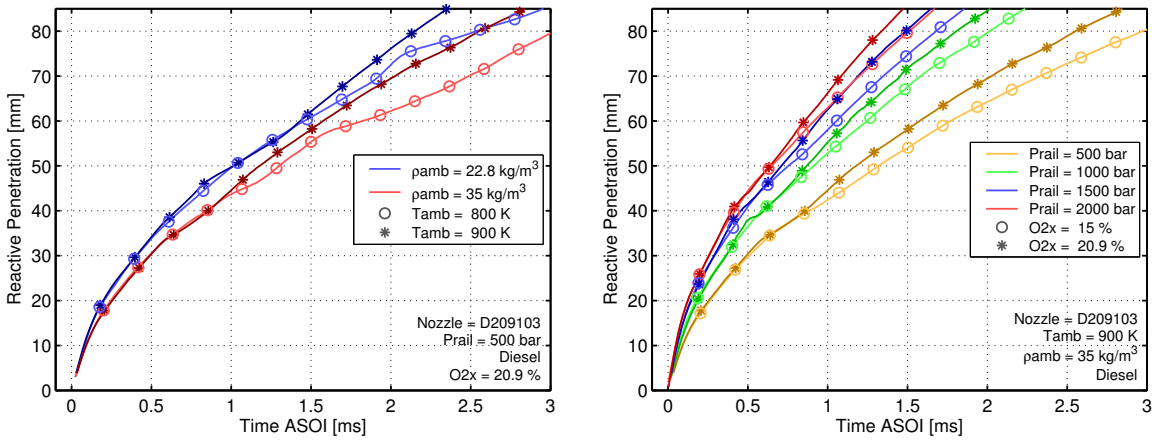

Fig. 6: Tip penetration measured at different conditions. Left: Influence of ambient density and temperature being observed at p_{rail} = 500 bar and O_2% = 20.9%. Right: Effect of injection pressure and oxygen concentration at T_{amb} = 900 K, ρ_{amb} = 35 kg/m^3. (Nozzle = Spray D, Fuel = Diesel). Color darkening represent temperature and O_2% increment for left and right plots respectively.

increased when oxygen concentration is increased. Comparing both plots, it is appreciable that temperature and oxygen percentage in atmosphere differently affect the growing behavior of the penetration although both influences seem to be related only to the combustion and they appear just when the ignition happens. Also, in Fig. 7 a direct comparison between different fuels sprays is depicted, where it can be seen how the spray development is similar before the combustion takes place. In the second pair of images, n-dodecane ignition has started while diesel has not yet. In the third pair, diesel spray is between the SoCF and the SSI, phase in which the spray tip gets transparent as a consequence of the cool flames onset. From fourth to sixth set of images, SSI has already occur and can be appreciated how n-dodecane penetration gets higher than diesel one.

In order to analyze this behaviors, it would be interesting to study penetration in terms of *R-parameter*. However, and contrary to the inert case, for reactive sprays is not so simple to express tip penetration with an unique $\overline{R}$ because of its different pattern, which is not constant along time. A sample of that can be appreciated in Fig. 8 top row plots, where reactive tip penetration presents a 'bump' and slope variations after that, which are related with the moment when the ignition takes place and the conditions under which it occurs. This temporal acceleration of spray agrees to the stages of combustion development described in [13], where it is stated that there is a short-lived peak in penetration ratio that rise from *SoCF*. The bump in penetration curve corresponds to this stage and is followed by a short deceleration and then a progressive acceleration phase until a quasi-steady ratio value [10]. Nevertheless, this can be noticed in terms of transient R as represented in Fig. 8 bottom row graph, where it can be seen that there is a first phase after the start and stabilization of the injection in which R presents a pseudo-constant pattern, similar to that should follow a jet under inert conditions. Following as reference the R evolution of Spray D - dodecane at O_2% = 20.9% (Fig. 8-right-bottom plot, dark curve with cross symbol), shortly after 0.7 ms ASOI starts an evident rise in which the ignition delay occurs. After a maximum near the 0.85 ms, a 'valley zone' begins, where the spray reduces and increases its advancement speed until a quasi-stable R phase after 1.3 ms ASOI. Last, this R value is greater than the stable one reached in the first before-reaction phase, which indicates that besides the acceleration obtained in the bump, the spray in the stable zone of combustion is also faster than in its first steady phase.

A significant parameter that controls the reactive penetration development seems to be the speed at which combustion reactions take place or, in other words, the ignition delay. Although the *ID* is treated more deeply in its respective subsection, this fact makes pertinent certain comparisons to be made. In first place, for same conditions, *ID* is shorter for n-dodecane than for diesel, which is predictable due to its higher tendency to auto-ignite, reflected in the cetane number of both fuels. Furthermore, R shows a longer valley zone for diesel than for n-dodecane. It can explain why in Fig. 8 top row, diesel and n-dodecane penetrations diverge significantly even with different slopes until up to 80 mm. This behavior also can be seen in high temperature tests, as Fig. 7 shows. Furthermore, it is well known how an O_2% increment shortens the ignition delay, but in Fig. 8 it can be observed that Spray C seems to be less sensitive to this effect than Spray D.

The authors attributed the aforementioned effect of valley zone prolongation in diesel to the difference of ignition delay between this fuel and n-dodecane. Comparing injection events for both fuels or for another dis-

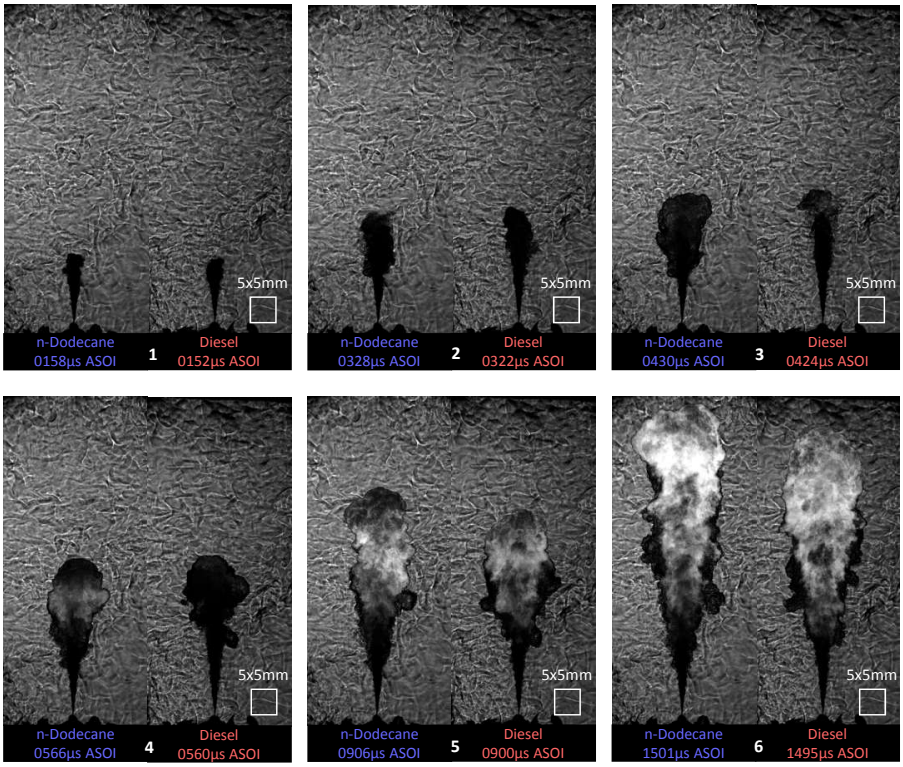

Fig. 7: Schlieren visualization sample of n-dodecane vs. diesel spray evolution. (Nozzle = Spray C, T_{amb} = 900 K, ρ_{amb} = 22.8 kg/m^3, p_{rail} = 1500 bar, O_2% = 20.9%). Note the time gap between both fuels images despite the camera records at the same speed, due to the difference between SOIs

similar *ID* conditions such as different temperatures, it is possible to note how the gaseous front formed when combustion takes place grows larger and slightly wider for later *ID* injections (diesel spray in Fig. 7), due to the longer time elapsed before ignition that ensures that a higher fuel mass have been injected and allows a better gas-fuel mixing and a broader gas expansion. The valley zone in R is a ralentization in the spray as a result of the gases of the heading front which are opposing to the fuel momentum flux not involved in the autoignition until being surpassed by it, which takes longer for larger expanded gas concentrations.

Given the importance of the *ID* and the way in which combustion takes place in reactive penetration, it can be assumed that ambient temperature is also a notable influential parameter. Fig. 9 shows how as discussed in non-reactive atmosphere (O_2% = 0 %), temperature has a negligible effect on tip penetration and R is substantially constant once the spray stabilizes. On other hand, in combustion experiments can be seen the *R-parameter* stages mentioned above (a non-reactive zone, followed by a peak or bump, a valley zone where R decays under the previous 'inert' values and rises continuously and finally, a quasi-steady zone). Fig. 9 supports which can also be noticed in Fig. 8, that is the higher the oxygen percentage, the greater the peak region maximum. Moreover, the last stable R of reactive tests reaches very similar values for all T_{amb} and O_2%, but higher than non-reactive tests values. This means that after spray enter in this quasi-steady condition (close to 1.7 ms in Fig. 9-right) penetration goes forward with slopes ($\partial S_v/\partial\sqrt{t}$) near to each other. However, Fig. 9-left shows how different is the spray progress at the end of the reactive curves, which can be better understood seeing R plot. In Fig. 8 bottom row and Fig. 9 right part, it can be appreciated how the spike in the spray acceleration have a higher max value with oxygen amount, which gives faster bump phases to the O_2% = 20.9 % tests; and also this stage tends to occur earlier (being bounded with ignition delay), allowing the reactive spray to reach its quasi-steady higher velocity sooner, and to outstrip the spray with lower oxygen concentrations.

Concerning to the ambient temperature influence, its increase causes an opposite effect on R than the first aforementioned but accentuates hugely the second one. In other words, the bump is smaller and has a shorter duration for higher temperatures because the prompt start of combustion does not allow to mix as properly and uniformly as at lower T_{amb}. However, this effect of the significant reduction in *ID* is broadly less important in

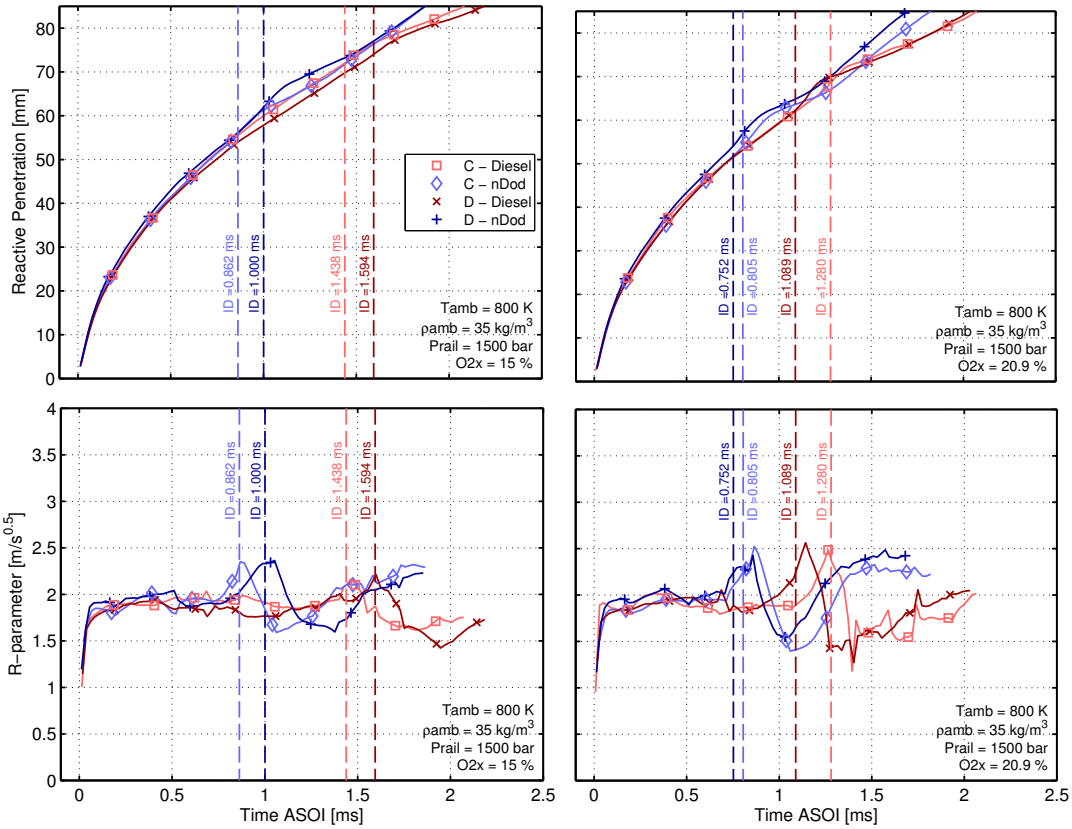

Fig. 8: Reactive tip penetration and R results for all nozzle-fuel combinations for different oxygen percentages. Dashed lines represent the ignition delay in each test. Up: Reactive Tip penetration measures. Down: Calculated R. Left: Experiment performed at $O_2\%$ = 15%. Right: Test at $O_2\%$ = 20.9%. Please note the different penetration and time scales between both parts (T_{amb} = 800 K, ρ_{amb} = 35 kg/m^3, p_{rail} = 1500 bar).

penetration than the shortening in the delay to reach the last stable and faster region and, as consequence, the increment in its duration for high-temperature sprays, granting them a considerable advantage over colder jets in penetration terms, noticeable in Fig. 9 left plot.

3.2. Ignition delay

From Fig. 10 it can be inferred that *ID* is a parameter susceptible to change with all the injection conditions varied in this work consistently with another researches [15, 17, 28, 32]. Ignition delay is largely influenced by chemistry and mixing processes. An increase in oxygen concentration, ambient density or temperature leads to an acceleration of the reactions of oxidation, causing an *ID* shortening. An ignition delay reduction is also sensitive to occur with injection pressure increments, which promotes turbulence, intensifying break-up and air-fuel mixing and facilitating combustion occurrence.

Fig. 10-left, agrees with these enunciations, showing how the gas temperature and $O_2\%$ dependency of *ID* are quite higher than density dependency in consonance with [28]. On the other hand, Fig. 10 right part shows the influence of injection pressure in *ID*, which is possibly comparable with oxygen concentration effect; and also thanks to the multiple p_{rail} points in test matrix, it can be appreciated how its effect is lower at higher pressures and at higher temperatures, being noticeable that the p_{rail} influence is quite weaker at 900 K than at 800 K. Another noticeable matter in Fig. 10 is the fuel influence on ignition delay, which is regularly higher for diesel than n-dodecane tests. This can be explained by comparing both fuels cetane number (Table 2), which give a measure of how quickly the fuel starts to burn under diesel engine conditions. Being higher for n-dodecane, it is expected that this is more prone to self-ignite than diesel, resulting in a shorter *ID*.

Nevertheless, the effect of different nozzles in ignition delay is difficult to see clearly in Fig. 10. In both plots appear that, for 800 K tests, *ID* is greater for Spray C than Spray D for same fuel at 15% oxygen percentage, but

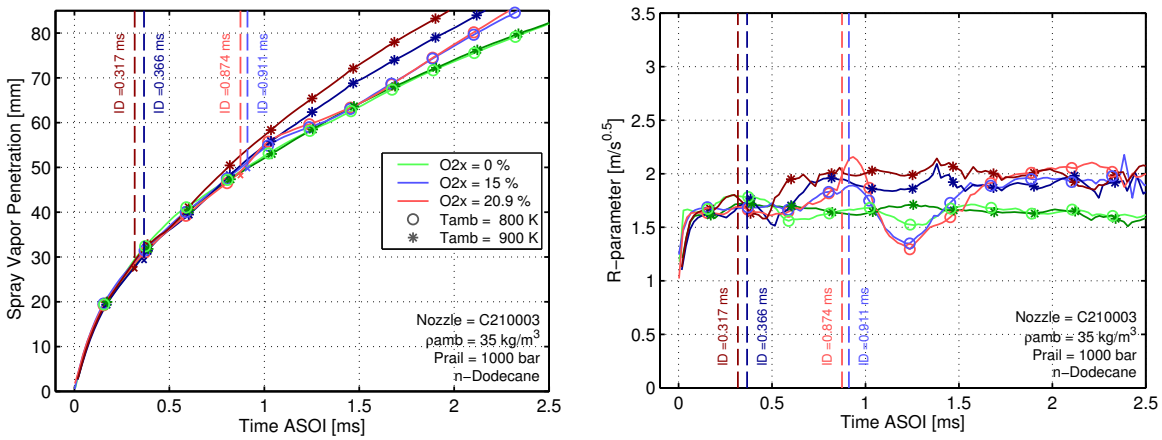

Fig. 9: Temperature and oxygen percentage effect on reactive axial spray advancement in terms of penetration and R. Left: Tip penetration of spray vapor phase and flame. Right: *R-parameter* at same conditions. Dashed lines represent the ignition delay in each reactive test (Nozzle = Spray C, Fuel = n-Dodecane, ρ_{amb} = 35 kg/m^3, p_{rail} = 1000 bar). Color darkening represent temperature increment.

at 20.9% the opposite happens systematically, which can be also seen in Fig. 8. However, at 900 K conditions, *ID* seems to be predominantly higher for Spray C. To aid to understand this behavior, Fig. 11 shows two *Ignition Delay ASOI vs. Oxygen Percentage* graphs at different injection pressures. Although only measurements at two different O_2% have been made, and the behavior of the ignition delay with oxygen concentration is not linear [17, 28], this figure gives some interesting information on its behavior. First, at 800 K it is clear how O_2% reduces *ID* for all nozzles, but with different strength. The slopes corresponding to Spray D are notably more pronunciated than Spray C slopes, which means that Spray C is less sensitive to undergo changes in ignition delay with O_2%, which was mentioned in *Tip penetration and R-parameter* section and is quite worthy to note. A possible explanation of this phenomenon is that for a cavitating nozzle as Spray C, the spray angle tends to be higher[22, 26], enlarging the jet volume and increasing the entrainment of air into the jet. This enhancement in air-fuel mixing rate reasonably reduces the decreasing ratio of *ID* with the oxygen molar fraction, in a form that does not occur for Spray D. Also, the slopes for both sprays tend to be quite more coincident at 900 K, where nozzle geometry seems to have insignificant effect.

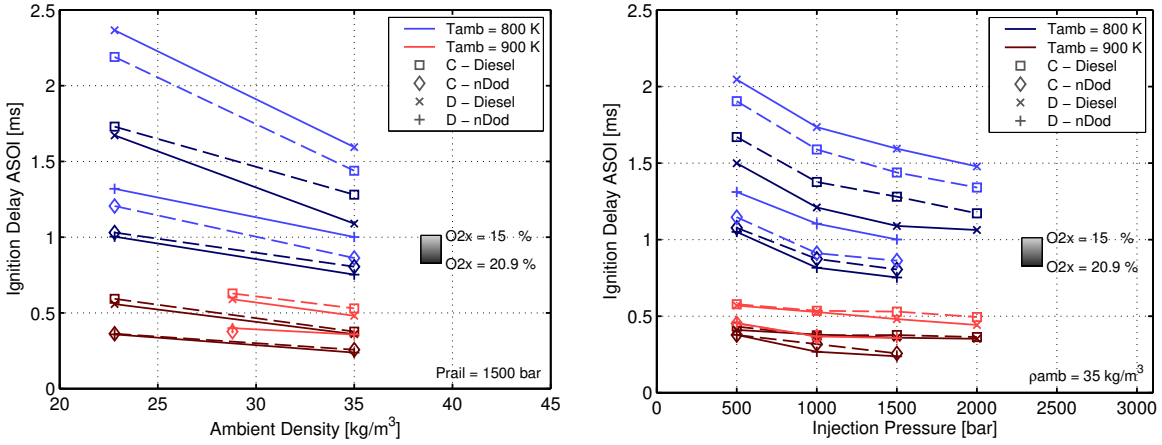

Fig. 10: Ignition delay variation with injection conditions at certain fixed parameters. Left: Ignition delay being affected by ambient density, temperature and oxygen concentration (p_{rail} = 1500 bar). Right: Injection pressure, gas temperature and oxygen concentration effect on ignition delay (ρ_{amb} = 35 kg/m^3). Dashed lines represent Spray C trends while continuous line is for Spray D.

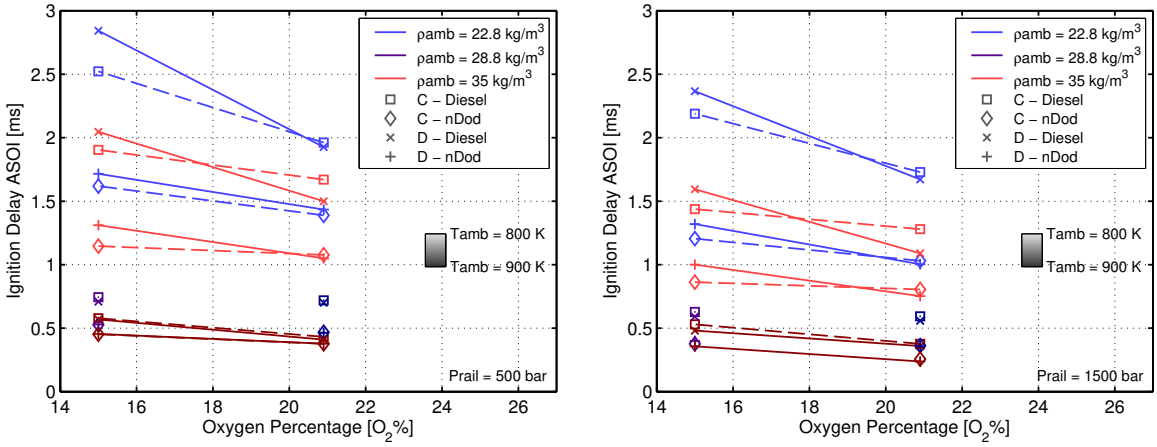

Fig. 11: Ignition delay variation with oxygen concentration for different injection pressures. Left: Experiments at p_{rail} = 500 bar. Right: Experiments at p_{rail} = 1500 bar. Dashed lines represent Spray C trends while continuous line is for Spray D.

Fig. 11 slopes also show remarkable tendencies (again knowing that not entirely represent the nonlinear behavior of *ID*). In both plots, at lower densities, Spray C and Spray D lines tend to be less inclined and intercept each other later than at higher densities, which means that the effect of oxygen concentration in *ID* and its sensitivity difference between nozzles weakens with density increments. This can also be seen increasing injection pressure (comparing both 11 plots). Fig. 11 reiterates how injection pressure effect on *ID* is nearly imperceptible at high temperatures compared with 800 K.

3.3. Lift-off Length

Following the previously described criteria, lift-off length was calculated, whose partial results can be observed in Fig. 12 as a function of ambient density and injection pressure (left and right part respectively). Several researches [14, 15, 18, 27] support the influence of this two parameters in *LOL*. Gas density, being a parameter that enhances the evaporation and mixing processes, causes a reduction in lift-off length. On the other hand, and contrary to the case of ignition delay, lift-off length is increased with higher injection pressures due to the fact that, the greater the jet velocity is, the further the flame front stabilizes. Such as density, gas temperature promote the evaporation and mixing formation so, even in a greater extent, reduce lift-off length as shows Fig. 12 according with [28]. Respect to oxygen concentration, it is visible how shortens the *LOL* because its consequence in laminar flame speed, following the concept proposed by Peters in [27]. These *LOL* behavior with parametric variations accords with the scaling law given by Pickett et al. in [17] (Equation 3), where Z_{sto} is the stoichiometric mixture fraction and u_{inj} is the outlet jet velocity, proportional to the square root of the difference between both injection and chamber pressures ($\sqrt{\Delta p}$).

$$LOL \propto T_{amb}^{-3.74} \cdot \rho_{amb}^{-0.85} \cdot Z_{sto}^{-1} \cdot D_o^{0.34} \cdot u_{inj} \tag{3}$$

Previous studies demonstrate that *LOL* is affected by fuel ignition quality, and fuels with higher cetane numbers (i.e. shorter ignition delays) commonly have shorter lift-off length [17, 33]. This corresponds with results obtained for diesel and n-dodecane in this experience. For same operating conditions, the *LOL* tendency for the different nozzles is generally the same that was observed in the Part I of this work for inert penetrations in both liquid and vapor phases: For n-dodecane, lift-off length is higher for Spray D than Spray C, while the opposite happens for diesel. Authors attribute this pattern to reasons similar to those that promote it for non-reactive penetrations [22], considering how lift-off length is reasonably well correlated with jet penetration [34] and the coefficient trends of these injectors visible in [26]. Dodecane, being less viscous, must develop a higher Reynolds number and velocity[35]. In a cavitating regime as the induced by the Spray C nozzle, this high *Re* will increment the turbulence through the nozzle and the cavitation, enhancing the jet break-up, enlarging the spray angle and dropping the coefficient of area, or the effective diameter [36, 37]. This reduction in the effective diameter will diminish the *LOL* that can be reached. On the other hand, Spray D is a nozzle designed to suppress cavitation, so the area coefficient will barely change by variations of Reynolds number. However, *Re* will increase the velocity

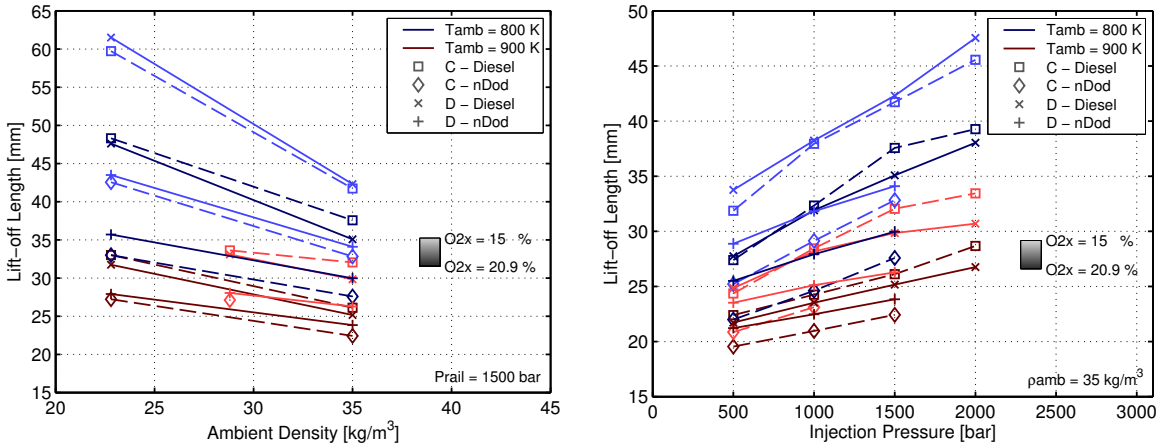

Fig. 12: Lift-off length variation with injection conditions at certain fixed parameters. Left: Ambient density, temperature and oxygen concentration effect on *LOL* (p_{rail} = 1500 bar). Right: Injection pressure, gas temperature and oxygen concentration effect on *LOL* (ρ_{amb} = 35 kg/m^3). Dashed lines represent Spray C trends while continuous line is for Spray D.

coefficient, and consequently also the outlet velocity of the spray u_{inj} whereby, according with Equation 3, will make lift-off higher. On the other hand, diesel is a more viscous fuel, developing a lower *Re* than n-dodecane at same injection conditions. This fact makes the greater outlet diameter of Spray C nozzle against Spray D, a dominant factor to increase *LOL* facing the diminished cavitation and its effects in area coefficient.

4. Conclusions

In the present work, the effects of injection condition variations, nozzle geometry, and employed fuel over the tip penetration and combustion parameters, such as ignition delay and lift-off length were studied, in reactive atmosphere. In the same way as in the first part of this research, in all tests points the penetration derivative respect to the square root of time, presented as *R-parameter*, was calculated. The experiments were performed with diesel and n-dodecane and for two different single-hole nozzles from the Engine Combustion Network, whose design is oriented to promote or suppress cavitation, respectively in case of Spray C and D; leading to the following conclusions:

- *R-parameter* was not constant with time, contrasting with inert experience, but it presented a systematic behavior for all tests which can be divided in the following phases: a constant zone before ignition, an accelerating bump due to the expansion produced when ignition takes place, a valley zone of acceleration decreasing-increasing, where R decays under the value of the constant zone, and finally, a quasi-steady region whose stable value is higher than the one in the zone before ignition. Furthermore, it was shown how the values and the duration of these characteristic phases depends in great matter of the ignition delay, ambient temperature and oxygen concentration, which in turn, will affect the reactive spray penetration, unlike the inert case where the only influencers between the evaluated parameters are the ambient density and the injection pressure. Those two parameters showed to affect penetration similarly in reactive cases.

- The steady value of *R-parameter* reached by the reactive spray after stabilize, is not affected by the oxygen concentration nor the gas temperature. Its parametric dependence is similar to the one which would have under non-reactive conditions, being influenced mainly by greater injection pressure and ambient density, increasing and decreasing with them respectively. However, it is important to highlight that this stable R value is higher than the attained by an inert spray.

- Fuel changing showed to affect all measured parameters, especially lift-off length and ignition delay, which successively affected reactive penetration. n-Dodecane values of *ID* and *LOL* were shorter due to its higher cetane number and autoignition quality respectively than diesel, but the viscosity of each fuel also played a notable role in the behavior of lift-off lengths, affecting it differently depending on the nozzle employed. For the conical Spray D nozzle, Reynolds number (higher for the less viscous fuel at same other conditions)

increased the velocity and how far could *LOL* get. In contrast, for Spray C nozzle, *Re* promoted the cavitating regime, giving rise to a faster liquid breakup and a reduction in effective diameter, and resulting in a limitation of the spray and lift-off length growth.

- The trend of ignition delay between nozzles did not change with fuel alike the *LOL* case, but with oxygen concentration. Spray C showed less sensitivity to O_2% increments as a product of the improvement in the air entrainment into the spray because its higher spreading angle induced by cavitation.

5. Acknowledgments

This work was supported by "Ministerio de Economía y Competitividad" of the Spanish Government in the frame of the projects "Estudio de la interacción chorro-pared en condiciones realistas de motor" , Ref. TRA2015-67679-c2-1-R. Moreover, the optical equipment employed in the project was purchased with investment from Ministerio de Economía y Competitividad FEDER-ICTS-2012-06.

The authors would finally like to thank Alberto Viera and Borja Hurtado for their collaboration in the setup of the experiments and laboratory work.

6. References

[1] I. Roisman, L. Araneo, C. Tropea, Effect of ambient pressure on penetration of a diesel spray, International Journal of Multiphase Flow 33 (2007) 904–920. doi:10.1016/j.ijmultiphaseflow.2007.01.004.

[2] C. Genzale, R. Reitz, M. Musculus, Effects of spray targeting on mixture development and emissions formation in late-injection low-temperature heavy-duty diesel combustion, Proceedings of the Combustion Institute 32 (2009) 2767–2774. doi:10.1016/j.proci.2008.06.072.

[3] M. Costa, U. Sorge, L. Allocca, Increasing energy efficiency of a gasoline direct injection engine through optimal synchronization of single or double injection strategies, Energy Conversion and Management 60 (2012) 77–86. doi:10.1016/j.enconman.2011.12.025.

[4] R. Payri, F. Salvador, J. Gimeno, V. Soare, Determination of diesel sprays characteristics in real engine in-cylinder air density and pressure conditions, Journal of Mechanical Science and Technology 19 (2005) 2040–2052. doi:10.1007/BF02916497.

[5] R. S. Baert, P. J. Frijters, B. Somers, C. C. Luijten, W. de Boer, Design and operation of a high pressure, high temperature cell for HD Diesel spray diagnostics: guidelines and results, SAE Technical Paper 2009-04-20 (2009). doi:10.4271/2009-01-0649.

[6] M. Meijer, B. Somers, J. Johnson, J. Naber, S.-Y. Lee, L. M. Malbec, G. Bruneaux, L. M. Pickett, M. Bardi, R. Payri, et al., Engine Combustion Network (ECN): Characterization and comparison of boundary conditions for different combustion vessels, Atomization and Sprays 22 (2012). doi:10.1615/AtomizSpr.2012006083.

[7] M. Bardi, R. Payri, L. M. Malbec, G. Bruneaux, L. M. Pickett, J. Manin, T. Bazyn, C. Genzale, Engine Combustion Network: comparison of spray development, vaporization, and combustion in different combustion vessels, Atomization and Sprays 22 (2012). doi:10.1615/AtomizSpr.2013005837.

[8] ECN, Engine Combustion Network, Online, 2015. URL: www.sandia.gov/ecn/.

[9] A. Kastengren, F. Tilocco, C. Powell, J. Manin, L. M. Pickett, R. Payri, T. Bazyn, Engine Combustion Network (ECN): Measurements of nozzle diameter and hydraulic behavior, Atomization And Sprays 22 (2012) 1011–1052. doi:10.1615/AtomizSpr.2013006309.

[10] J. M. Desantes, J. Pastor, J. García-Oliver, F. Briceno, An experimental analysis on the evolution of the transient tip penetration in reacting diesel sprays, Combust. Flame 161 (2014) 2137–2150. doi:10.1016/j.combustflame.2014.01.022.

[11] L. M. Pickett, S. Kook, T. C. Williams, Visualization of diesel spray penetration, cool-flame, ignition, high-temperature combustion, and soot formation using high-speed imaging, SAE Technical Paper 2009-01-0658 (2009). doi:10.4271/2009-01-0658.

[12] J. V. Pastor, R. Payri, J. M. García-Oliver, J. G. Nerva, Schlieren Measurements of the ECN-Spray A Penetration under Inert and Reacting Conditions, SAE Technical Paper 2012-01-0456 (2012). doi:10.4271/2012-01-0456.

[13] R. Payri, J. M. García-Oliver, T. Xuan, M. Bardi, A study on diesel spray tip penetration and radial expansion under reacting conditions, Applied Thermal Engineering 90 (2015) 619–629. doi:10.1016/j.applthermaleng.2015.07.042.

[14] J. Benajes, R. Payri, M. Bardi, P. Martí-Aldaraví, Experimental characterization of Diesel ignition and lift-off length using a single-hole ECN injector, Applied Thermal Engineering 58 (2013) 554 – 563. doi:10.1016/j.applthermaleng.2013.04.044.

[15] R. Payri, J. P. Viera, Y. Pei, S. Som, Experimental and numerical study of lift-off length and ignition delay of a two-component diesel surrogate, Fuel 158 (2015) 957–967. doi:10.1016/j.fuel.2014.11.072.

[16] D. L. Siebers, B. Higgins, Flame lift-off on direct-injection diesel sprays under quiescent conditions, SAE Technical Paper 2001-01-0530 (2001). doi:10.4271/2001-01-0530.

[17] L. M. Pickett, D. L. Siebers, C. A. Idicheria, Relationship between ignition processes and the lift-off length of diesel fuel jets, SAE Technical Paper 2005-01-3843 (2005). doi:10.4271/2005-01-3843.

[18] O. O. Taskiran, M. Ergeneman, Effect of nozzle dimensions and fuel type on flame lift-off length, Fuel 115 (2014) 833–840. doi:10.1016/j.fuel.2013.03.005.

[19] D. Guyot, F. Guethe, B. Schuermans, A. Lacarelle, C. O. Paschereit, CH*/OH* chemiluminescence response of an atmospheric premixed flame under varying operating conditions, in: Proceedings of ASME Turbo Expo 2010: Power for Land, Sea and Air, Glasgow, UK, 2010. doi:10.1115/GT2010-23135.

[20] H. Persson, O. Andersson, R. Egnell, Fuel effects on flame lift-off under diesel conditions, Combust Flame 158 (2011) 91–97. doi:10.1016/j.combustflame.2010.07.020.

[21] L. M. Pickett, S. Kook, H. Persson, O. Andersson, Diesel fuel jet lift-off stabilization in the presence of laser-induced plasma ignition, Proc Combust Inst 32 (2009) 2793–2800. doi:10.1016/j.proci.2008.06.082.

[22] J. Gimeno, G. Bracho, P. Martí-Aldaraví, J. E. Peraza, Experimental study of the injection conditions influence over n-dodecane and diesel sprays with two ECN single-hole nozzles. Part I: Inert atmosphere, Energy Conversion and Management 126 (2016) 1146–1156. doi:10.1016/j.enconman.2016.07.077.

[23] D. Siebers, Liquid-phase fuel penetration in Diesel sprays, SAE Technical Paper 980809 (1998). doi:10.4271/980809.

[24] R. Payri, J. M. García-Oliver, M. Bardi, J. Manin, Fuel temperature influence on diesel sprays in inert and reacting conditions, Applied Thermal Engineering 35 (2012) 185–195. doi:10.1016/j.applthermaleng.2011.10.027.

[25] R. Payri, J. Gimeno, M. Bardi, Study liquid length penetration results obtained with a direct acting piezo electric injector, Applied Energy 106 (2013) 152–162. doi:10.1016/j.apenergy.2013.01.027.

[26] R. Payri, J. Gimeno, J. Cuisano, J. Arco, Hydraulic characterization of diesel engine single-hole injectors, Fuel 180 (2016) 357–366. doi:10.1016/j.fuel.2016.03.083.

[27] N. Peters, Turbulent Combustion, Cambridge Monographs on Mechanics, Cambridge University Press, 2000. doi:10.1017/CBO9780511612701.

[28] B. Higgins, D. Siebers, Measurement of the flame lift-off location on DI diesel sprays using OH chemiluminescence, SAE Technical Paper 2001-01-0918 (2001). doi:10.4271/2001-01-0918.

[29] A. Gaydon, The Spectroscopy of Flames, Springer Netherlands, 2012. doi:10.1007/978-94-009-5720-6.

[30] R. Payri, J. Gimeno, J. P. Viera, A. H. Plazas, Needle lift profile influence on the vapor phase penetration for a prototype diesel direct acting piezoelectric injector., Fuel 113 (2013) 257–265. doi:10.1016/j.fuel.2013.05.057.

[31] J. M. Desantes, R. Payri, F. Salvador, A. Gil, Development and validation of a theoretical model for diesel spray penetration, Fuel 85 (2006) pp. 910–917. doi:10.1016/j.fuel.2005.10.023.

[32] M. Lapuerta, J. Sanz-Argent, R. R. Raine, Ignition Characteristics of Diesel Fuel in a Constant Volume Bomb under Diesel-like Conditions. Effect of the Operation Parameters, Energy & Fuels 28 (2014) 5445–5454. doi:10.1021/ef500535j.

[33] O. Kuti, J. Zhu, K. Nishida, X. Wang, Z. Huang, Characterization of spray and combustion processes of biodiesel fuel injected by diesel engine common rail system, Fuel 104 (2013) 838–846. doi:10.1016/j.fuel.2012.05.014.

[34] M. K. Bobba, Flame Stabilization and Mixing Characteristics in a Stagnation Point Reverse Flow Combustor, Ph.D. thesis, Georgia Institute of Technology, 2007.

[35] G. Jiang, Y. Zhang, H. Wen, G. Xiao, Study of the generated density of cavitation inside diesel nozzle using different fuels and nozzles, Energy Conversion and Management 103 (2015) 208–217. doi:10.1016/j.enconman.2015.06.065.

[36] R. Payri, F. J. Salvador, J. Gimeno, O. Venegas, Study of cavitation phenomenon using different fuels in a transparent nozzle by hydraulic characterization and visualization, Experimental Thermal and Fluid Science 44 (2013) 235–244. doi:10.1016/j.expthermflusci.2012.06.013.

[37] F. J. Salvador, J. Martínez-López, C. Caballer, M.and De Alfonso, Study of the influence of the needle lift on the internal flow and cavitation phenomenon in diesel injector nozzles by cfd using rans methods, Energy Conversion and Management 66 (2013) 246–256. doi:10.1016/j.enconman.2012.10.011.